Astron. Astrophys. 363, 289–294 (2000)

ASTRONOMY AND ASTROPHYSICS

Correlative relationships in an inhomogeneous solar atmosphere

A.S. Gadun[1,†], **A. Hanslmeier**[2], **A. Kučera**[3], **J. Rybák**[3], **and H. Wöhl**[4]

[1] Main Astronomical Observatory of Ukrainian NAS, Goloseevo, 03680 Kiev-127, Ukraine
[2] Institut für Geophysik, Astrophysik und Meteorologie, Universitätsplatz 5, 8010 Graz, Austria
[3] Astronomical Institute, Slovak Academy of Sciences, 05960 Tatranská Lomnica, Slovakia
[4] Kiepenheuer-Institut für Sonnenphysik, Schöneckstrasse 6, 79104 Freiburg, Germany

Received 17 February 2000 / Accepted 17 August 2000

Abstract. We analyse the correlative relationships between various quantities derived from 2-D inhomogeneous and time-dependent model atmospheres and between selected simulated line parameters to compare them with height-dependent correlations derived from spectral observations. We detect three photospheric regions: thermal convection, overshooting convection and a transition layer. We also show that correlations found for the model data and those computed within simulated spectral observations are a good testing tool for line formation depths. As an example, we examine two criteria, providing heights of line core formation in LTE, and conclude that the approach which defines this quantity as geometrical height at line center optical depth $\tau_{\lambda 0}$ = 1 is likely more suitable for diagnostic purposes than the method based on depression contribution function.

Key words: Sun: granulation – Sun: photosphere – hydrodynamics – line: formation

1. Introduction

The solar photosphere can be treated as a transition region between thermal convection, which predominates below the surface and in the low photosphere (overshooting convection) and different kinds of oscillations, which completely define the gas dynamics in the upper layers.

In this context, it was studied in a large number of papers – for instance, among others, by Leighton et al. (1962), Evans (1964), Krat (1973), Canfield & Mehltretter (1973), Keil & Canfield (1978), Kneer et al. (1980), Durrant & Nesis (1981, 1982), Nesis et al. (1988), Komm et al. (1990, 1991a, 1991b), Karpinsky (1990), Hanslmeier et al. (1990, 1994), Balthasar et al. (1990), Kučera et al. (1995). Since the correlation analysis is the simplest method to extract information concerning the global behaviour of physical quantities in the photospheric medium, it was widely used in most these studies (e.g. Karpinsky 1990 and references therein).

Send offprint requests to: A. Hanslmeier (arh@bimgs1.kfunigraz.ac.at)
† deceased

In the paper of Espagnet et al. (1995) the height variation of the solar granulation was investigated using a 16-min time series of two– dimensional (2-D) multichannel subtractive double pass spectrograms in the NaD_2 5690 line obtained at the Pic du Midi Observatory. Krieg et al. (1999) used Fabry-Perot interferometer data obtained at the Vacuum Tower Telescope at the Observatorio del Teide to analyze spectral scans of narrow-band images across the NaD_2 line. They found that granular intensity fluctuations occur in the deep photosphere only and disappear at heights of about 100 km. Contrary to Krieg et al., Espagnet et al. found an intensity pattern visible in the upper photosphere which is of turbulent origin.

On the other hand, multidimensional hydrodynamic (HD) simulations of solar granulation have reached a high level of realism. They reproduce a significant number of observables (Stein & Nordlund 1998, Gadun et al. 1999, Asplund et al. 2000, Georgobiani et al. 2000, Ploner et al. 2000) but they were never involved for a detailed investigation of the photospheric structure. Exceptions are the papers of Gadun et al. (1997 and 1999), who reproduced correlations between line parameters within 2-D model atmospheres.

In this paper we want to employ both the correlation analysis and 2-D model atmospheres to study the photospheric structure. We shall deal with three groups of correlations.

Into the first group we include the model (or theoretical) correlations. They describe correlations between selected quantities of 2-D model atmospheres. These correlations are derived directly from time-dependent 2-D models.

To test spectral observations for diagnostic purpose is another aim of this paper. For this reason, we have made an analysis of spectrograms obtained from 2-D models. They have been also studied in the context of correlation analysis. These correlations between simulated line parameters form the second group of correlative relationships, presented here. We shall call them the simulated correlations.

Finally, we test our simulations by comparing the model and simulated correlations with those provided by real spectral observations. We use the spectral observations made with high spatial and spectral resolution. These correlative dependencies will be called the observed correlations in the following. The third group of our correlations contains these quantities.

We show that the result of this comparison as well as the application of spectral line diagnostics are sensitive to the method providing an estimation of line formation depths and briefly analyse two criteria to calculate them.

2. 2-D models and spectral observations

The 2-D models used here and the limitations of a 2-D approach were described by Gadun et al. (1999) in detail. The models have a computational box with sizes 3360 km × 1960 km in horizontal and vertical directions (the atmospheric layers occupy about 700 km). The spatial step is 28 km.

2-D models normally produce larger model oscillations than 3-D simulations. Therefore in these simulations special boundary conditions at the top and at the bottom of the computational domain were chosen such that the oscillations were kept as weak as possible. These conditions were described by Gadun et al. (1999). The total evolution time of the simulated granulation which was taken into consideration in our analysis is about $2^h\ 22.5^m$. The time step between the studied models is 30 s.

The spectral observations were described in detail by Kučera et al. (1995) and Hanslmeier et al. (2000). They were carried out with the Vacuum Tower Telescope (Observatorio del Teide, Tenerife) using its echelle spectrograph. Five Fe I spectral lines have been observed strictly simultaneously with exposure time of 0.3 s: 5434.543 Å, 6494.994 Å, 5576.508 Å, 6301.508 Å, and 6302.499 Å. Their main characteristics are given in Kučera et al. (1995). The slit width was 0.28″ and the subsequent spectral profiles are separated by to 0.17″ in the spatial direction. The dispersions of the spectra were between 3.3 and 4.0 mÅ/px. Only the most quiet region covering 30arcsec on the Sun was used for the computation of the continuum intensity and the spectral line characteristics (the residual line core intensity and the Doppler shifts). This region was without supergranular network activity and was situated close to the disk center ($\mu > 0.95$).

3. Theoretical correlative relationships

In this section we present height-dependent correlative relationships derived from 2-D models. In particular, we shall deal with two different sorts of correlations. The first of them is called a two-component representation, when thermodynamic quantities are averaged over up- and downflows, separately. Such relationships can be directly compared with the results, produced by inversion codes (Bellot Rubio et al. 1999, Frutiger et al. 1999, for instance). The second kind of correlations are linear correlation coefficients which reflect the linear dependence of model quantities between each other. These correlative dependencies were studied in a large number of papers using observations of spectral lines formed at various heights in the photosphere.

3.1. Two-component representation

Fig. 1 shows temperature, gas pressure and density fluctuations averaged over up- and downflows, separately, and over the total evolution time. Hereafter, the surface level or h = 0 in the geometrical height scale corresponds to log $\overline{\tau_R}$ = 0, where $\overline{\tau_R}$ is the Rosseland optical depth averaged over time and space in our sequence of 2-D models.

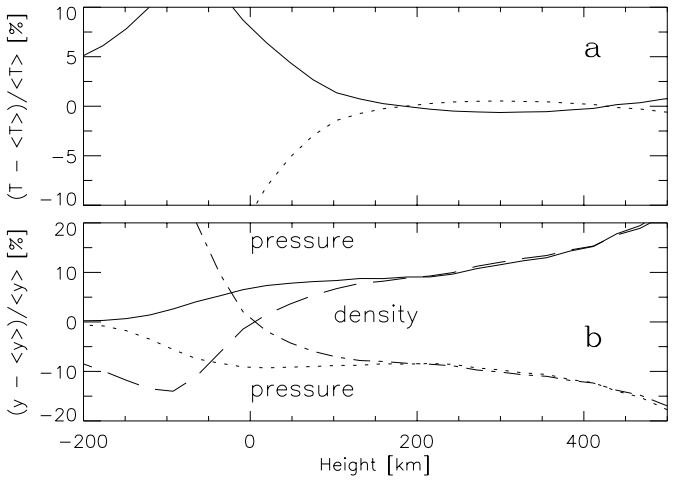

Fig. 1a and b. Relative temperature **a**, pressure and density **b** fluctuations in two-component representation: the quantities were averaged over up- and downflows, separately. The temperature and gas pressure in upflows are shown by solid lines. Dotted lines denote temperature and gas pressure in downflows. The dashed line marks the averaged density in upflows and the dotted-dashed line is mean density in downflows.

From Fig. 1a we can clearly see two crucial height levels where temperature fluctuations reverse their sign. The first reversal (Nelson & Musman 1977) occurs at $h \sim 170$ km and is caused by a cooling of thermal convective upflows which overshoot into stable photospheric layers and a heating of downflows due to their compression. Near the traditional temperature minimum there exists the second reversal of temperature fluctuations – oscillating upflows are seen to be hotter again due to compression of the medium as they move into the upper atmospheric layers. Such a behaviour of temperature fluctuations is very similar in 2-D models and in the output of inversion codes (Bellot Rubio et al. 1999, Frutiger et al. 1999).

Fig. 1b exhibits the pressure and density averaged inside up- and downflows and shown as relative variations around their mean values at certain height levels. They outline three regions:

- convectively unstable subphotospheric layers (negative correlation between density and vertical velocity),
- a region of overshooting convection (correlation between density and vertical velocity becomes positive but $|\Delta P|/\overline{P}$ is significantly greater than $|\Delta\rho|/\overline{\rho}$ and $\Delta T/\overline{T}$ is positive (negative) in upflows (downflows),
- and oscillating photospheric layers being in radiative equilibrium ($\Delta P/\overline{P} \approx \Delta\rho/\overline{\rho}$).

Based on these models we may conclude that overshooting convection extends to about 150–170 km in the photosphere. However, this extension of the overshooting convection region, varies in dependence on the size of the convective cell: for instance, above cells with horizontal sizes of about 180 km it only extends to below 70–75 km (Gadun et al. 2000).

3.2. Correlative relationships

We analyse two kinds of correlations: one- and two-point correlations. The one-point (local) correlations correspond to correlation coefficients calculated between spatial variations of model quantities at the same model (horizontal) layer. Two-point correlations were found between spatial fluctuations of model quantities when one point is fixed around the surface level and the other point will be taken at various heights. These correlations reflect changes in the columnar structure of the inhomogeneous atmosphere.

We have determined the correlations between model quantities or between selected line parameters for each model. The mean correlation coefficients are obtained by averaging over the modeling time interval or over the time interval of observations.

3.2.1. Two-point correlations

We start our analysis with correlations between δI (spatial variations of emergent monochromatic intensity at λ 500 nm) and spatial variations of temperature fluctuations at each horizontal level i in the photosphere (δT_i). They again demonstrate a high correlation (Fig. 2) in the low photosphere, dropping rapidly with height and becoming even negative at h larger than 120–130 km. This occurs due to the first reversal of temperature fluctuations inside the photospheric columnar structure (Fig. 1a): overcooling of the matter above the central part of the convective cells and heating of gas above intercellular lanes. The largest anticorrelation is found in the middle photosphere at heights between 250 and 350 km, where the reversal of temperature fluctuations is most pronounced (Fig. 1a). At these heights the temperature fluctuations are almost a mirror image of the granular brightness field. In the upper photosphere this anticorrelation decreases but is still significant in spite of the second reversal of temperature fluctuations because oscillations and shearing flows break down the quasi columnar structure there. In the Figs. 2–4 we have used $n = 285$ models.

The correlations between δI and spatial variations of vertical velocities (δW_i) demonstrate another dependence on height: they decrease slowly from a high level of correlation in the low photosphere to almost zero level at or near the traditional temperature minimum, there is no reversal field of vertical velicities.The high correlation between δI and δW_i becomes smaller than 0.5 at a height of about 250 km.

$\langle \delta I, \delta P g_i \rangle$ and $\langle \delta I, \delta \rho_i \rangle$ (correlations between δI and fluctuations of gas pressure and density, respectively) correspond to those as to be expected in the transition region from thermal convection to layers with radiative equilibrium. For instance, $\langle \delta I, \delta \rho_i \rangle$ are in anticorrelation in subphotospheric layers – less dense matter is hotter and brighter as well, but in optically thin layers they become positive due to the buoyancy breaking effect.

The peak in height dependence of $\langle \delta I, \delta P g_i \rangle$ is located around the surface, i.e. deeper than for the $\langle \delta I, \delta \rho_i \rangle$ stratification, and positive over almost the whole photosphere.

Let us comment on of the correlations between δI and $\delta \kappa_5$ (spatial variations of monochromatic opacity at λ 500 nm). In the low photosphere, where temperature fluctuations are larger, they follow the $\langle \delta I, \delta T_i \rangle$ but in high photospheric layers $\delta \kappa_5$ almost coincides with spatial fluctuations of gas pressure. This is explained by the sensitivity of H^- ions to electron concentrations; H^- ions constitute the main absorber in the solar atmosphere. In the low photosphere, the electron concentration depends mainly on hydrogen ionization which is strongly temperature-dependent. However, in higher layers the metals are the main contributor. Since the metals are basically ionized due to the still high temperatures, the electron concentration in these layers is not very sensitive to temperature fluctuations.

In Fig. 3 we present a series of two-point correlations in which we use a profile of vertical (δW_{-60}) and horizontal

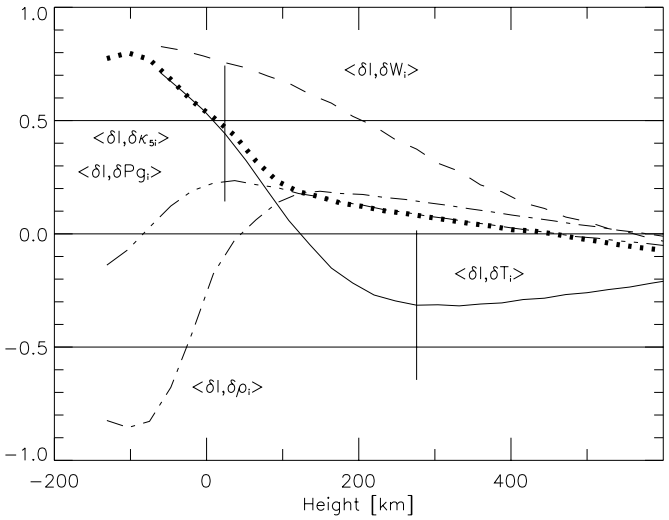

Fig. 2. Correlations between monochromatic emergent intensity at λ 500 nm and selected model quantities derived at various height levels in the model photosphere. Error bars given as $x \pm \sigma$ indicate the scatter in values.

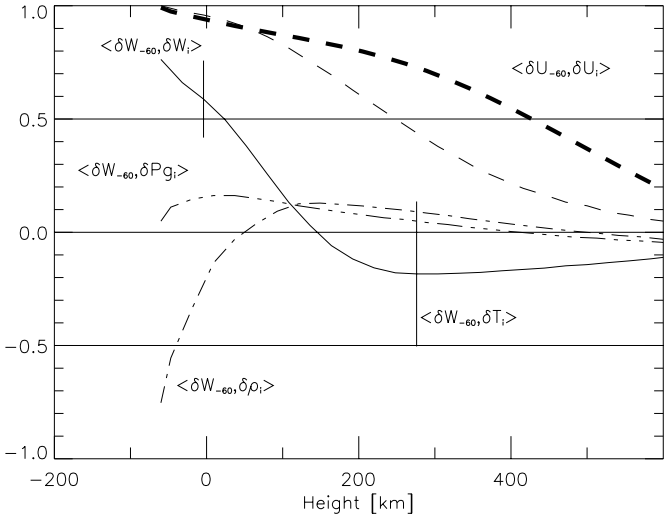

Fig. 3. Correlations between vertical velocity fluctuations at a depth 60 km below the surface and selected model quantities as well as correlations between horizontal velocities $< \delta W_{-60}, \delta W_i >$ (dashed line). The error bars are standard deviations shown as $x \pm \sigma$.

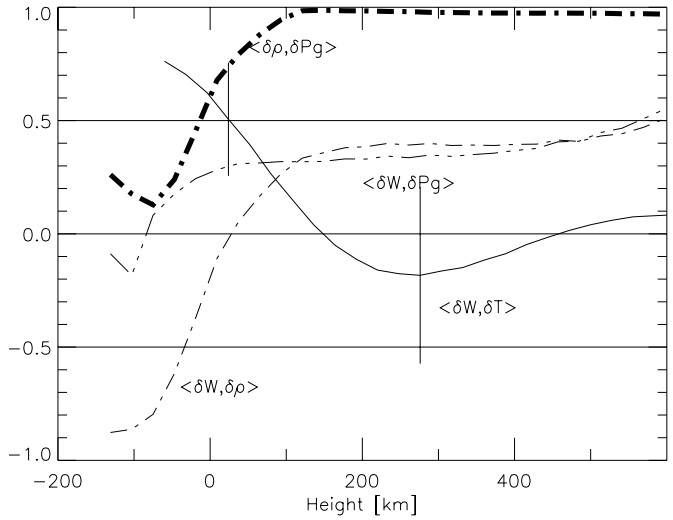

Fig. 4. Local correlations between spatial fluctuations of selected model quantities. Error bars are estimates of standard deviations which are given as $x \pm \sigma$.

(δU_{-60}) velocities at a depth of 60 km below the surface. They can serve as better indicators of the columnar structure of the model photosphere than correlations with δI.

Correlations with (δW_{-60}) show almost the same behaviour as the correlation coefficients with δI previously discussed. $\langle \delta W_{-60}, \delta T_i \rangle$, however, exhibit positive correlation over a larger geometrical height range than $\langle \delta I, \delta T_i \rangle$. It is important that horizontal velocities are highly correlated in these models over almost the whole photosphere. We note that from obvious reasons the correlation of spatial fluctuations of horizontal velocities with δI or δW_{-60} is absent (is close or equal to zero).

3.2.2. One-point correlations

The one-point (local) correlations are given in Fig. 4. They show the correlation coefficients found between selected model quantities for each horizontal level.

The correlation $\langle \delta W, \delta T \rangle$ demonstrates, as mentioned above, two reversals of temperature fluctuations in the model atmosphere and a large anticorrelation due to overcooling of thermal convective flows in optically thin layers. We may also note the relatively large positive correlations between vertical velocities and $\delta\rho$ and δPg: on the average, ascending flows produce denser atmospheric inhomogeneities which have higher pressure than downflows. $\delta\rho$ and δPg are highly correlated over the whole model atmosphere.

δW and $\delta\rho$ are negatively correlated up to a height of about 30 km. This may serve as an argument that the top of thermal convection reaches the low photosphere. The same conclusion is followed from Figs. 1–3.

The positive $\langle \delta W, \delta T \rangle$ correlation in the upper photosphere does not change significantly the negative values of $\langle \delta I, \delta T_i \rangle$ and $\langle \delta W_{-60}, \delta T_i \rangle$ because the photosphere does not have a columnar structure in the upper layers.

Table 1. Spectral lines used for simulation.

λ Å	El.	EPL eV	H_d km	H_{ew} km	H_τ km
4911.536	Fe I	4.26	148	126	45
6494.499	Fe I	4.73	155	131	71
6495.740	Fe I	4.83	165	132	89
4911.782	Fe I	3.93	181	148	121
5679.032	Fe I	4.65	197	151	158
6496.472	Fe I	4.79	204	155	162
5543.944	Fe I	4.22	215	168	183
6027.059	Fe I	4.07	230	174	185
6481.878	Fe I	2.28	266	217	222
6280.622	Fe I	0.86	303	246	253
5250.216	Fe I	0.12	330	277	308
5250.654	Fe I	2.20	352	292	406
6494.994	Fe I	2.40	414	308	492
5136.800	Fe II	2.84	94	84	23
5100.656	Fe II	2.81	99	85	32
5425.259	Fe II	3.20	128	105	89
6432.683	Fe II	2.89	141	115	89
4576.339	Fe II	2.84	186	148	177
5234.630	Fe II	3.22	238	176	233

4. Comparison with line parameter correlations

Theoretical correlations $\langle \delta I, \delta T_i \rangle$, $\langle \delta I, \delta W_i \rangle$, and $\langle \delta W, \delta T \rangle$ can be compared with results of spectral observations made with high spatial resolution, namely with correlations $\langle \delta I, \delta r \rangle$, $\langle \delta I, \delta V \rangle$, and $\langle \delta V, \delta r \rangle$, if we suppose that a) we know exactly the region of the atmosphere where the spectral line is formed and b) if the region which contributes mainly to the line formation process is narrow. Both assumptions are supported by results of Kučera et al. (1998). Here δr denote spatial variations of residual intensity in the line core and δV correspond to spatial variations of Doppler shifts.

To test whether spectral lines reproduce the main real correlative relationships of the model photosphere we simulated a set of 13 Fe I and 6 Fe II lines using our time-dependent 2-D models. The line parameters are given in Table 1. Together with line wavelength (λ) and low excitation potential (EPL), Table 1 represents an estimation of line formation heights. H_{ew} denotes the effective height of line formation for the line equivalent width (weighted over the whole profile); H_d is the effective height of line formation for central line depth; H_τ is the geometrical height at line center optical depth $\tau_{\lambda 0} = \tau_{\lambda 0}^{c+l}$ = 1.0. Here $\tau_{\lambda 0}^{c+l}$ denote the integral optical depth in the line and in the continuum at the wavelength of the line center. H_{ew} and H_d were calculated with depression contribution and Unsöld-Pecker weighting functions. All these weighting quantities we computed for a 1-D model which was obtained by spatially and temporally averaging our sequence of 2-D models.

Fig. 5 displays correlations, derived from these simulations. They are shown in dependence on H_d (Fig. 5a–c) and H_τ (Fig. 5d–f). If we compare between $\langle \delta I, \delta W_i \rangle$ and $\langle \delta I, \delta V \rangle$

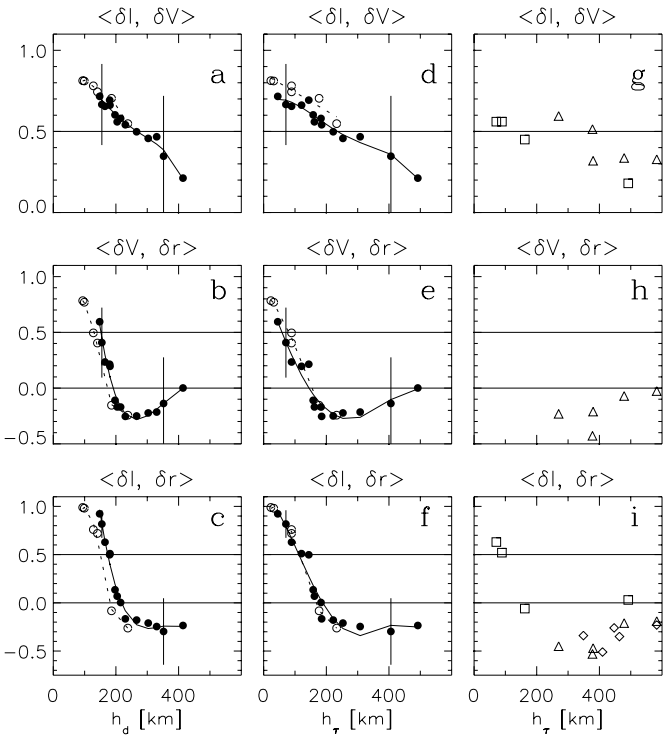

Fig. 5a–i. Correlations found from simulated **a–f** and observed **g–i** variations. Error bars are estimates of the standard deviations – they reflect a scatter of the correlation coefficients measured from the set of spectrograms. The open circles and dashed lines represent Fe II lines, filled circles with solid lines are correlations obtained with Fe I lines. The squares stem from Fe I observations of Hanslmeier et al. (1990); triangles from Fe I observations of Kučera et al. (1995) and those presented here; and diamonds from Fe I lines investigated by Balthasar et al. (1990).

(Fig. 2 – Fig. 5a and d), $\langle \delta W, \delta T \rangle$ and $\langle \delta V, \delta r \rangle$ (Fig. 4 – Fig. 5b and e), and $\langle \delta I, \delta T_i \rangle$ and $\langle \delta I, \delta r \rangle$ (Fig. 2 – Fig. 5c and f) it is easy to conclude that a) spectral line correlations correctly reproduce real correlative relationships of the model atmosphere if b) we use the H_τ scale of geometrical heights for our sample of spectral lines. Therefore, this scale is more suitable for diagnostic purpose in the context of our 2-D models.

To test these simulated correlations we present in Figs. 5g–i correlation coefficients calculated for five Fe I lines from spectral observations described in Sect. 2. The numerical values of correlations are given in Table 2 where means and differences have been derived from two subsequent exposures taken in the same slit position. The height H_τ, determined in the same way as in Table 1, is given in Table 2 too. Moreover in Figs. 5g–i some previously published data are plotted from papers of Hanslmeier et al. (1990), Balthasar et al. (1990), and Kučera et al. (1995).

Although these observations do not describe possible relationships in detail, they are not in disagreement with the theoretical prediction. It is very important that $\langle \delta V, \delta r \rangle$ show a tendency to decrease their negative correlative relationship in the upper photosphere in agreement with model predictions.

Table 2. Correlations of the spectral line characteristics derived from the observations.

λ Å	H_τ km	$\langle \delta I, \delta V \rangle$	$\langle \delta V, \delta r \rangle$	$\langle \delta I, \delta r \rangle$
6302.499	270	0.60±0.08	−0.23±0.06	−0.45±0.03
6301.508	378	0.51±0.10	−0.43±0.06	−0.53±0.06
5576.099	380	0.32±0.09	−0.21±0.07	−0.47±0.05
6494.994	492	0.34±0.12	−0.07±0.14	−0.21±0.16
5434.543	583	0.33±0.13	−0.03±0.13	−0.19±0.13

5. Discussion and conclusion

The height dependencies of the model correlations will change if we use another method to calculate mean correlation coefficients: we may collect data belonging to each horizontal level over a whole time series of our models and then calculate correlations between these data. But the height dependencies of the new correlations differ from those discussed in this paper not more than by 20–30 km and this does not change significantly our main conclusions.

From our simulated spectral observations we do not detect the sharp drop of correlation between spatial fluctuations of vertical velocities in the low and in the middle photosphere as it was reported by Karpinsky (1990). An explanation can be that our models are obviously more laminar than the real solar photosphere. However, this conclusion of Karpinsky was not confirmed later.

Our results with high correlation between horizontal velocities in the model photosphere are also in disagreement with a study of Nesis et al. (1988), where they found, based on observations, that horizontal velocities are coherent only in the low photosphere. We do not exclude that our model result could be influenced by the 2-D cartesian approach, close to laminar treatment of the medium, and spatially limited computational domain.

In spite of this the correlations derived from observations and from simulations of several Fe I and Fe II lines are in good agreement. Therefore, summarizing our results we may conclude that:

a) almost in the whole photosphere above granules the matter predominantly ascends.
b) clouds of cold and dense matter are located above bright granules beginning from heights about 150–170 km;
c) above 250 km the columnar structure of the photosphere is broken down.

Schematically, the structure of the model photosphere can be presented as the following:

a) low photosphere: it seems that the top of the thermal convection zone lays at 20–50 km above the visible surface;
b) then we have convection overshoot into stable layers up to 150–170 km;
c) between 170 and 250–300 km we detect a transition layer where the convective columnar structure still exists (due to

the influence of convective pressure variations) and where the inversion of temperature fluctuations is largest;

d) above 300 km this columnar structure is broken on the average and the photospheric medium is controlled mostly by oscillations.

This scheme agrees with the picture from spectral observations (Nesis et al. 1988, Karpinsky 1990).

Finally we point out that multidimensional selfconsistent model atmospheres can be successfully used to test possible criteria in estimation of "line formation depths". Although our results show that the H_τ scale seems to be better suited for diagnostic purpose than the line formation depths found with the depression contribution functions we suggest to test also physically more adequate methods using the conception of the response functions.

Acknowledgements. A. G. and A. H. thank the Austrian Academy of Sciences and the National Academy of Sciences of Ukraine for financing the exchange of scientists. A. H. thanks the 'Austrian Fonds zur Förderung der wissenschaftlichen Forschung' for supporting these investigations. A. K and J. R. acknowledge the grant VEGA 2/7229/20 and the Austrian and Slovak Academy of Sciences.

References

Asplund M., Nordlund Å., Trampedach R., Stein R.F., 2000, A&A, submitted
Balthasar H., Grosser H., Schröter C., Wiehr E., 1990, A&A 235, 437
Bellot Rubio L.R., Ruiz Cobo B., Collados M., 1999, A&A 341, L31
Canfield R.C., Mehltretter J.P., 1973, Solar Phys. 33, 33
Durrant C.J., Nesis A., 1981, A&A 95, 221
Durrant C.J., Nesis A., 1982, A&A 111, 272
Espagnet O., Muller R., Roudier Th., Mein N., Mein P., 1995, A&AS 109, 79
Evans J.W., 1964, Astroph. Norveg. 9, 33
Frutiger C., Solanki S.K., Bruls J.H.M.J., Fligge M., 1999, In: Nagendra K.N., Stenflo J.O. (eds.) Solar Polarization. Kluwer, Dordrecht, in press
Gadun A.S., Hanslmeier A., Pikalov K.N., 1997, A&A 320, 1001
Gadun A.S., Solanki S.K., Johannesson A., 1999, A&A 350, 1018
Gadun A.S., Ploner S.R.O., Hanslmeier A., et al., 2000, A&A, in preparation (also Gadun A.S., Solanki S.K., Ploner S.R.O., et al., 1998, Size-Dependent Properties of 2-D Artificial Solar Granulation, Main Astr. Obs., Kiev, preprint no. MAO-98-4E)
Georgobiani D., Kosovichev A.G., Nigam R., Nordlund Å., Stein R.F., 2000, ApJ 530, L139
Hanslmeier A., Mattig W., Nesis A., 1990, A&A 238, 345
Hanslmeier A., Nesis A., Mattig W., 1994, A&A 288, 960
Hanslmeier A., Kučera A., Rybák J., Neunteufel B., Wöhl H., 2000, A&A, 356, 308
Karpinsky V.N., 1990, In: Stenflo J.O. (ed.) Solar Photosphere: Structure, Convection, and Magnetic Fields. Kluwer, Dordrecht, p. 67
Keil S.L., Canfield R.C., 1978, A&A 70, 169
Kneer F.J., Mattig W., Nesis A., Werner W., 1980, Solar Phys. 68, 31
Komm R., Mattig W., Nesis A., 1990, A&A 239, 340
Komm R., Mattig W., Nesis A., 1991a, A&A 243, 251
Komm R., Mattig W., Nesis A., 1991b, A&A 252, 812
Krat V.A., 1973, Solar Phys. 32, 307
Krieg J., Wunnenberg M., Kneer F., Koschinsky M., Ritter C., 1999, A&A 343, 983
Kučera A., Rybák J., Wöhl H., 1995, A&A 298, 917
Kučera A., Balthasar H., Rybák J., Wöhl H., 1998, A&A 332, 1069
Leighton R.B., Noyes R.W., Simon G.W., 1962, ApJ 135, 474
Nelson G.D., Musman S., 1977, ApJ 214, 912
Nesis A., Durrant C.J., Mattig W., 1988, A&A 201, 153
Ploner S.R.O., Solanki S.K., Gadun A.S., 2000, A&A, in press
Stein R.F., Nordlund Å., 1998, ApJ 499, 914